European Journal of Neuroscience, Vol. 11, pp. 2403–2412, 1999

Expression in mammalian cells and electrophysiological characterization of two mutant Kv1.1 channels causing episodic ataxia type 1 (EA-1)

Frank Bretschneider, Anja Wrisch, Frank Lehmann-Horn and Stephan Grissmer
Department of Applied Physiology, University of Ulm, AlbertEinsteinAllee 11, D89081 Ulm, Germany

Keywords: EA1-associated mutations in Kv1.1, electrophysiology, episodic ataxia type 1, voltage-gated potassium channels, Kv1.1

Abstract

Episodic ataxia type 1 (EA-1) is a rare neurological disorder and was the first ionic channel disease to be associated with defects in a potassium channel. Until now 10 different point mutations in the KCNA1-gene have been reported to cause this disorder. We have investigated the functional consequences of two mutations leading to amino acid substitutions in the first and sixth transmembrane segments of a Kv1.1 channel subunit, by means of the patch-clamp technique; we injected cRNA coding for, respectively, F184C and V408A mutant Kv1.1 channels into mammalian cells and compared the resulting currents with those in the wild-type. The expression levels of F184C and V408A mutant channels relative to that of the wild-type was 38 and 68%, respectively. Since the single-channel conductance of the F184C mutant was similar to that of the wild-type (12 pS) without an apparent change in the maximum open probability, we conclude that the lower expression level in the F184C mutant channels is due to a reduced number of functional channels on the cell surface. F184C activated slower, and at more depolarized potentials, and deactivated faster compared with the wild-type. V408A channels deactivated and inactivated faster compared with the wild-type. Studies with different extracellular cations and tetraethylammonium gave no indication that the pore structure was changed in the mutant channels. Acetazolamide, that is helpful in some patients suffering from EA-1, was without effect on Kv1.1 wild-type or mutant channels. This study confirms and extends earlier studies on the functional consequences of Kv1.1 mutations associated with EA-1, in an attempt to understand the pathophysiology of the disease.

Introduction

The clinically and genetically heterogeneous group of hereditary paroxysmal ataxias could be divided into several groups. One particular group was first recognized by van Dyke *et al*. (1975) who described a disease in a family with an autosomal dominant mode of inheritance, later called EA-1. Besides the signs of a cerebellar dysfunction, all patients exhibited continuous myokymia during the, mostly brief, attacks. Later, these main symptoms of ataxia during attacks, and muscular signs between attacks, were confirmed in other families. Generalized ataxia and, in some cases, jerking movements, trembling or shaking limbs, are mostly brought on by startle, sudden movements after rest or exertion, and are influenced by illness, stress, fatigue, hunger, menses or anxiety. Facultative aura-like symptoms, such as the sensation of falling, blurred vision, weakness of the legs or vertigo suggested that cerebral systems other than the cerebellum might be affected (VanDyke *et al*., 1975; Hanson *et al*., 1977; Gancher & Nutt, 1986; Brunt & van Weerden, 1990; Lubbers *et al*., 1995). First ataxic episodes will usually be recognized in patients between the ages of 2 and 15 years (VanDyke *et al*., 1975; Brunt & van Weerden, 1990) and the frequency of attacks (from > 15 attacks per day to a few per year) tend to attenuate after the age of 20 years (Lubbers *et al*., 1995). Continuous muscle rippling – preferentially in distal muscles, muscle cramps or spasms could be detected in every affected person, at least after provocation by (limb) ischaemia (Brunt & van Weerden, 1990; Lubbers *et al*., 1995). Repetitive duplets, triplets or multiplets underlying the continuous muscle activity have been consistently found by means of electromyography over periods of months. These repetitive discharges, and also bursts of irregular frequency, were generated in peripheral motor neurons (Brunt & van Weerden, 1990).

Linkage studies in EA-1 families followed by sequencing of candidate genes led to the discovery of heterozygous point mutations in highly conserved regions of a delayed rectifier potassium channel, Kv1.1 (Browne *et al*., 1994, 1995; Litt *et al*., 1994; Comu *et al*., 1996; Scheffer *et al*., 1998). Figure 1 illustrates schematically the positions of the mutations in one Kv1.1 protein known, so far, to cause EA-1.

The Kv1.1 protein is localized in a variety of brain regions including cerebral cortex, bulbus olfactorius, hippocampus, retina, basal nuclei, thalamus, fibre tracts of the cerebrum and brain stem, and in regions affected in EA-1 as cerebellar nuclei, Purkinje, basket and granular cells of the cerebellum and juxtaparanodal regions of nodes of Ranvier of peripheral nerves (Beckh & Pongs, 1990; Klumpp *et al*., 1991; Roberds & Tamkun, 1991; Tsaur *et al*., 1992; Wang *et al*., 1993, 1994; Mi *et al*., 1995; Veh *et al*., 1995; Laube *et al*., 1996; Rhodes *et al*., 1997). By separate injection of cRNA-encoding human Kv1.1 channels with the six different point mutations described by Browne *et al*. (1994, 1995) into *Xenopus* oocytes, Adelman *et al*. (1995) were able express two of the mutants

Correspondence: Dr Stephan Grissmer, as above.
E-mail: stephan.grissmer@medizin.uniulm.de

Received 28 October 1998, revised 2 March 1999, accepted 4 March 1999

(F184C and V408A) with different electrophysiological properties compared with the wild-type. The other four cRNA (coding for V174F, R239S, F249I and E325D mutant channels) gave no currents when injected alone, and decreased currents when coinjected with the wild-type cRNA. Two types of cRNA (coding for R239S and E325D mutants channels) had a dominant negative effect on Kv1.1 currents. Later D'Adamo *et al*. (1998) and Zerr *et al*. (1998) were able to express V174F, F249I, E325D mutant Kv1.1 channels functionally in *Xenopus* oocytes, and described them electrophysiologically. The mutants showed differences in activation, deactivation and expression levels compared with the wild-type.

In our study we focused on the expression of two mutations in Kv1.1 channels responsible for EA-1, F184C and V408A, for the first time in mammalian cells and investigated them electrophysiologically. Only some of the electrophysiological properties are similar to the previously mentioned reports. Our study confirms and extends earlier studies on the functional consequences of Kv1.1 mutations associated with EA-1 in an attempt to understand the pathophysiology of the disease.

Some of the results have been reported in preliminary communications (Bretschneider *et al*., 1998).

Materials and methods

Cells

All experiments were carried out on single cells of a rat basophilic leukaemia cell line, RBL-cells (Eccleston *et al*., 1973). Cells were obtained from the American Type Culture Collection (Rockville, MD, USA). The cells were maintained in a culture medium of EMEM (Gibco, Berlin, Germany) supplemented with 1 mM L-glutamine (Biochrom, Berlin, Germany) and 10% heat-inactivated foetal calf serum (CCPRO, Karlsruhe, Germany) in a humidified, 5% CO_2 incubator at 37 °C. Cells were plated to grow non-confluently onto glass 1 day prior to use for injection and electrophysiological experiments (Rauer & Grissmer, 1996).

Solutions

The experiments were done at room temperature (21–25 °C). Cells were bathed, if not stated otherwise, in normal mammalian Ringer's solution containing (in mM): NaCl, 160; KCl, 4.5; $CaCl_2$, 2; $MgCl_2$, 1 and HEPES, 10, with an osmolarity of 290–320 mOsm. The pH was adjusted to 7.4 with NaOH. For permeation experiments and for some experiments to investigate deactivation bathing solutions contained (in mM): XCl, 164.5; (where $X = K^+$, Rb^+ or NH_4^+), $CaCl_2$, 2; $MgCl_2$, 1 and HEPES, 10, adjusted to pH 7.4 with XOH, with an osmolarity of 290–320 mOsm. A simple syringe-driven perfusion system was used to exchange the bath solutions in the recording chamber. The patch pipettes for the whole-cell and outside-out measurements were filled usually with a solution containing (in mM): KF, 135; $CaCl_2$, 1; $MgCl_2$, 2; HEPES, 10; EGTA, 10, adjusted to pH 7.2 with KOH, with an osmolarity of 290–320 mOsm. For determining inactivation of wild-type and V408A mutant Kv1.1 channels, 135 mM K-aspartate was used instead of 135 mM KF as internal solution.

Tetraethylammonium (TEA^+) was purchased from FLUKA Chemie AG (Buchs, Germany) as tetraethylammonium chloride. A TEA^+-stock solution was prepared containing (in mM): TEA^+, 160;

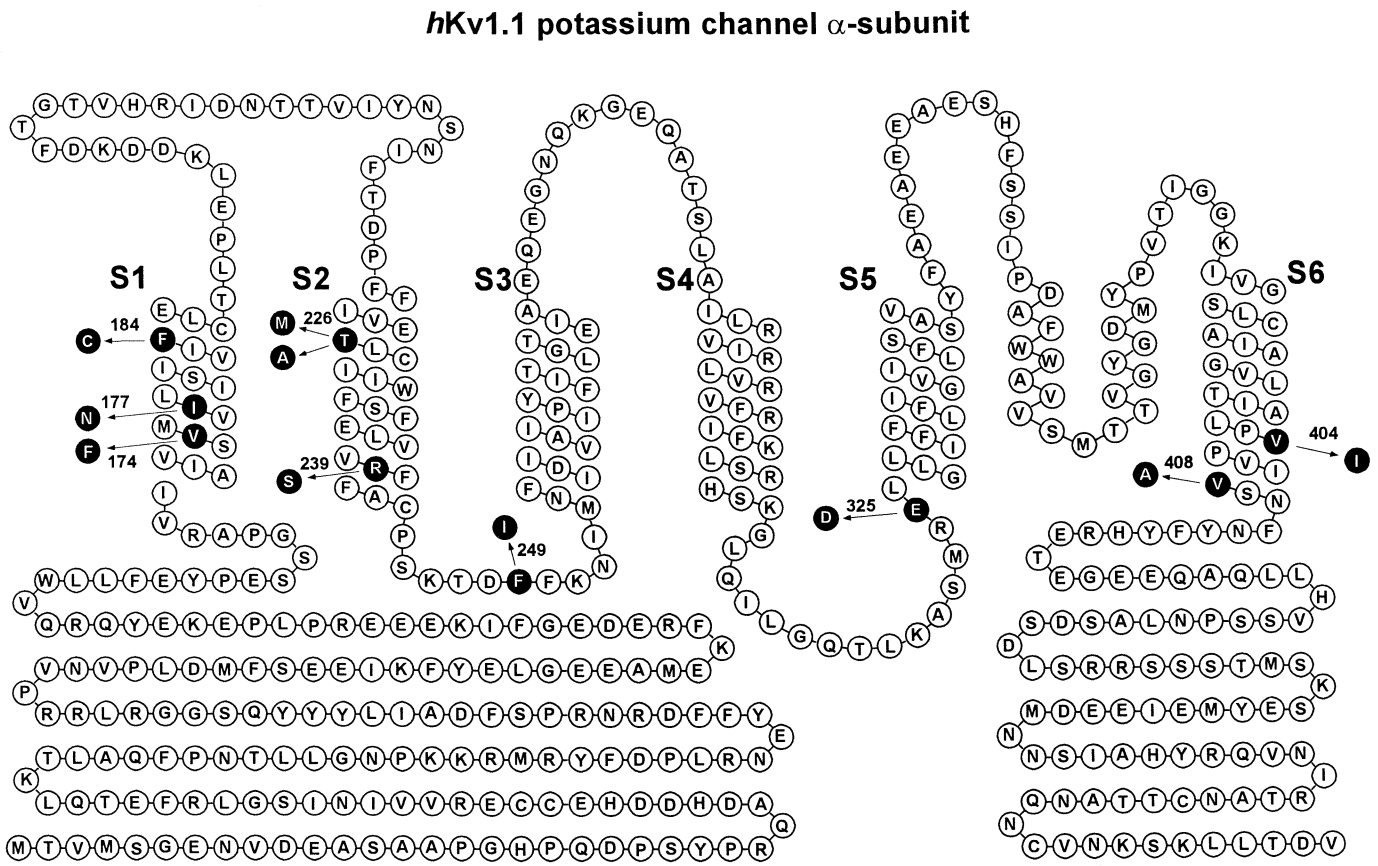

FIG. 1. Schematic representation of one Kv1.1 channel α-subunit. The mutations known to be associated with EA-1 are highlighted.

KCl, 4.5; $CaCl_2$, 2; $MgCl_2$, 1; HEPES, 10, from which dilutions were made in normal mammalian Ringer's solution to yield the 0.3 mM test solutions.

Acetazolamide was purchased from Aldrich Chemical Company, Inc. (Milwaukee, USA). Acetazolamide was added to normal mammalian Ringer's solution to get final concentrations of 1 mM.

Electrophysiology

Experiments were carried out using the whole-cell or outside-out configuration of the patch-clamp technique (Hamill *et al*., 1981) as described earlier (Grissmer *et al*., 1992a,b, 1993; Aiyar *et al*., 1994; Rauer & Grissmer, 1996; Jäger *et al*., 1998). Electrodes were pulled from glass capillaries (Clark Electromedical Instruments, Reading, UK) in three stages, coated with Sylgard (Dow Corning, Seneffe, Belgium) and fire-polished to resistances measured in the bath of 2.5–4 MΩ. Membrane currents were recorded with an EPC-9 patch-clamp amplifier (HEKA elektronik, Lambrecht, Germany) interfaced to a Macintosh computer running acquisition and analysis software (Pulse and Pulsefit). Cell capacitance was measured in the whole-cell configuration with the C_{slow} routine of Pulse following trains of square-wave pulses. Capacitative and leak currents were subtracted using the P/10 and, for 10 s depolarizing pulses, the P/4 procedures. Liquid junction potentials measured as described by Neher (1992) were < 3 mV and were not corrected for. The holding potential in all experiments was –80 mV. Filter frequency was normally 2.9 kHz, except for investigation of tail currents in V408A mutant Kv1.1 channels, where a filter frequency of 10 kHz was used.

For analysis of single-channel currents TAC (HEKA elektronik, Lambrecht, Germany) was used. Nonlinear approximations and presentation of data were performed using the program Sigmaplot (Jandel, Corte Madera, USA). Averaged data are given as mean values ± SD. Statistical significance was verified with an unpaired Student's *t*-test with $P < 0.01$.

Expression

The human Kv1.1 (*h*Kv1.1) gene (kindly provided by Dr M. Tanouye, Berkeley, USA) was subcloned into PBSTA plasmids normally containing the entire coding sequence of the *mouse* Kv1.1 gene (Chandy *et al*., 1990) after removal of the *m*Kv1.1 gene. PBSTA containing *h*Kv1.1 gene was linearized with Pst1 and transcribed *in vitro* with the T7 Cap-Scribe System (Boehringer Mannheim, Mannheim, Germany). The resulting cRNA was Phenol/Chloroform purified and could be stored at –75 °C for several months.

Injection

The cRNA was diluted with a fluorescent FITC-dye (0.5% FITC-Dextran in 100 mM KCl) to a final concentration of 1 µg/µL. RBL cells were injected with the cRNA/FITC-solution filled in injection capillaries (Femtotips®) using an Eppendorf microinjection system (Micromanipulator 5171 and Transjector 5246, Hamburg, Germany). In the visualized cells, specific currents were routinely measured 12–24 h after injection, in some cases 6–42 h after injection.

Generation of the F184C and V408A mutant hKv1.1 channels

For substituting phenylalanine at position 184 with cysteine and valine at position 408 with alanine, respectively, the QuikChange™ Site-Directed Mutagenesis Kit (Stratagene GmbH, Heidelberg, Germany) was used and the mutations were confirmed by sequencing single-stranded DNA with the Cy5-AutoRead Kit (Pharmacia, Uppsala, Sweden).

Results

Characterization of currents following injection of wild-type, F184C or V408A cRNA into mammalian cells

Expression

In order to determine the consequences of the two mutations responsible for EA-1, F184C and V408A, whole-cell currents were measured after separate injection of equal amounts of wild-type, F184C or V408A cRNA into rat basophilic leukaemia cells. We elicited outward currents after 100-ms-long depolarizations to 40 mV with a maximum of current of 516 ± 170 pA for wild-type, 93 ± 105 pA for F184C and of 335 ± 143 pA for V408A Kv1.1 channels, respectively (data not shown). Converting each current amplitude into a corresponding conductance and dividing the resulting conductances by cell capacitance (see Table 1) yielded

TABLE 1. Electrophysiological characteristics of Kv1.1 wild-type and mutant channels

	Wild-type *h*Kv1.1 channel		F184C *h*Kv1.1 channel		V408A *h*Kv1.1 channel	
Activation						
$E_{1/2}$ (mV)	–32 ± 4	(19)	–4 ± 5	(7)*	–31 ± 6	(11)
k (mV)	10 ± 2	(19)	10 ± 3	(7)	10 ± 1	(11)
τ_n at $E_{1/2}$ (ms)	5 ± 2	(9)	11 ± 2	(5)*	6 ± 2	(7)
Deactivation						
τ_t, at –70 mV (ms)	17.6 ± 5.3	(8)	8.8 ± 3.0	(6)*	0.8 ± 0.3	(4)*
τ_t at –100 mV in wild-type and V408A and –70 mV in F184C (ms)†	13.3 ± 2.7	(9)	8.8 ± 3.1	(6)	0.8 ± 0.3	(6)*
Inactivation						
τ_h at 40 mV (s)‡	11.4 ± 0.6	(5)	12 ± 1	(3)	3.6 ± 0.3	(5)*
Maximum conductance						
g_{max} (nS)	4.1 ± 1.4	(22)	1.6 ± 0.8	(13)*	2.7 ± 1.1	(15)*
Cell capacitance						
C_{cell} (pF)	18 ± 4	(22)	19 ± 5	(13)	19 ± 8	(15)
G_{max}/C_{cell} (S/F)	224 ± 42	(22)	86 ± 44	(13)*	153 ± 70	(15)*
Single-channel conductance						
γ (pS)	11.9 ± 0.8	(3)	12.5 ± 0.7	(3)		

Values given are mean ± SD, with the number of investigated cells in parenthesis. Maximum conductances, g_{max}, were usually derived from current-voltage relations (see Fig. 2). In some cases single depolarizations to 40 mV were used to calculate g_{max}. †In K^+-bathing solution. ‡In K^+-aspartate pipette solution; *Significantly different from wild-type value

values relative to the wild-type value of 38% and 68% for F184C and V408A Kv1.1 channels, respectively.

Activation

In order to characterize the activation of currents through wild-type, F184C and V408A Kv1.1 channels, families of current were elicited by 100-ms depolarizing pulses from –60 to 50 mV in 10-mV increments every 30 s (Fig. 2A). To determine the voltage dependence of activation, the peak currents from these records were converted into the corresponding conductances as described in the legend to Fig. 2B. To compare the voltage-dependent gating of each channel type, we normalized the conductances to the maximum conductance observed in the experiment (Fig. 2B). It is obvious from this diagram (Fig. 2B) that wild-type and V408A Kv1.1 channels activated at similar depolarization voltages with the value for half maximum activation ($E_{1/2}$), obtained from Boltzmann equations (see legend to Fig. 2B), of ~ –30 mV. The gradient of the voltage-dependence (k) was ~10 mV for all three channel types. The conductance–voltage relationship for F184C mutant channels, however, was shifted ~ 25 mV towards more depolarized potentials compared with wild-type Kv1.1 channels. The wild-type characteristics are similar to those of *m*Kv1.1 channels stably expressed in a mammalian cell line described earlier by Grissmer *et al.* (1994). Furthermore, the values for k and $E_{1/2}$ of all channel types are similar to values obtained when the channels were expressed in *Xenopus* oocytes (Adelman *et al.*, 1995; D'Adamo *et al.*, 1998; Zerr *et al.*, 1998; see also Table 1).

The voltage- as well as the time-dependence of activation of the Kv1.1 channel is important for its action in nerve cells. Therefore we were also interested in the time course of activation. From records similar to those in Fig. 2A we obtained activation time constants (τ_n) at different voltages using the n^4 Hodgkin–Huxley formula (see Hille, 1992). Means of these activation time constants were plotted against the depolarization voltages (see Fig. 2C). No differences of these voltage-dependent constants could be detected comparing wild-type and V408A Kv1.1 channels (Fig. 2C). The slower activation time constants observed in F184C channels were only partially due to the shift in the activation voltage as can be seen when comparing the mean values of the activation time constants of F184C with those of wild-type channels at $E_{1/2}$ (Table 1). These data are in agreement with previously published work using *Xenopus* oocytes as an expression system (Adelman *et al.*, 1995; D'Adamo *et al.*, 1998; Zerr *et al.*, 1998).

Deactivation

In additional experiments, we investigated the deactivation time course of currents through wild-type, F184C and V408A channels. We found deactivation of currents through V408A mutant channels to be very fast at voltages below –70 mV (approximately 0.1 ms at –100 mV; data not shown). To avoid errors in obtaining deactivation time constants from (small) inward currents at potentials more negative than the K^+ equilibrium potential (near –85 mV in normal mammalian Ringer's solution) we used another approach to characterize and compare the deactivation in wild-type and mutant channels. Swenson & Armstrong (1981) and later Cahalan *et al.* (1985) showed that the deactivation of potassium channels in squid axons and in T lymphocytes, respectively, was slowed down through

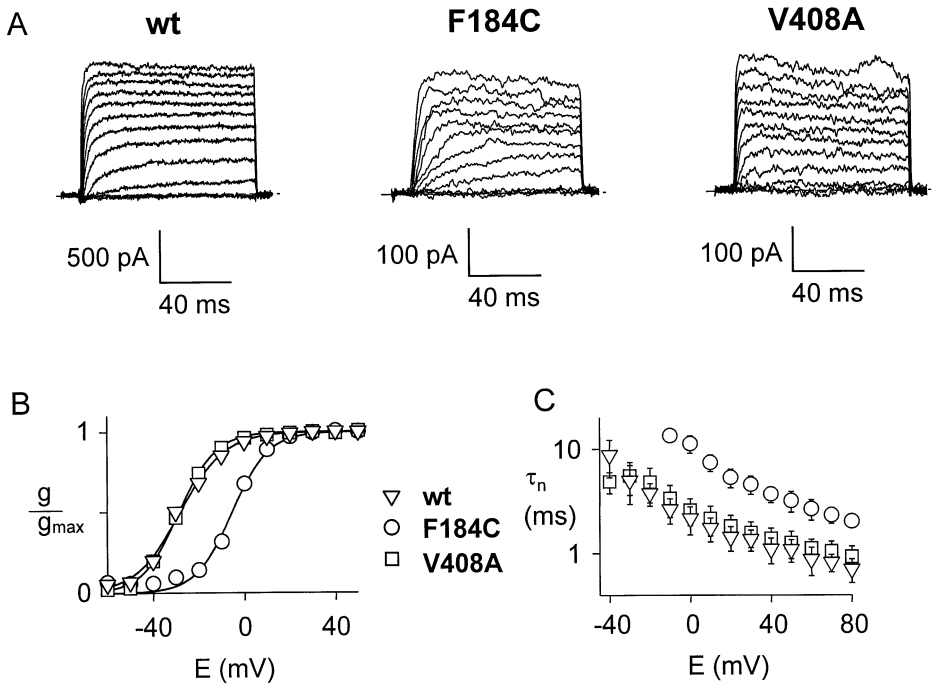

FIG. 2. Activation of currents through wild-type and mutant Kv1.1 channels. (A) Current traces were elicited in response to a set of 100-ms voltage steps from –60 to 50 mV in 10-mV increments every 30 s (B) Normalized conductances for the K^+ currents shown in A are plotted against the applied membrane potential E (mV). Peak K^+ conductances were obtained by dividing the peak K^+ currents by the driving force (applied membrane potential minus K^+ reversal potential, taken as –85 mV), and the resulting conductances g were than divided by the maximum conductance g_{max} at potentials > 20 mV to obtain normalized g. The lines through the points were fitted with the Boltzmann equation: $g/g_{max}(E) = 1/\{1 + \exp[(E_{1/2} - E)/k]\}$, with parameter values for the wild-type, F184C and V408A data of $E_{1/2} = -28.1, -5.3$ and -28.6 mV, respectively, and of $k = 10.0$, 9.1 and 9.0 mV, respectively. (C) The mean of the activation time constants (τ_n) ± SD from three to 14 cells for each type of channel (wild-type, F184C and V408A) were plotted against the depolarization potential. Currents were elicited similar to those in (A) but to 80 mV in 10 mV increments. Activation time constants τ_n were calculated with the n^4 Hodgkin–Huxley formala. However, at depolarizations more negative than –40 mV for wild-type and V408A and more negative than –10 mV for F184C, respectively, currents were in most cases too small to be fitted to obtain τ_n. In some cases, the SD was smaller than the symbol size used in this figure.

an increase in the extracellular potassium concentration. We obtained similar results in Kv1.1 wild-type channels as can be seen in Fig. 3. Substituting 160 mM Na^+ with K^+ slowed down the deactivation (see tail currents in Fig. 3A). To show this in more detail, monoexponential fits of the repolarization currents of the example in Fig. 3 were done and the resulting deactivation time constants were plotted against the repolarization voltage. Deactivation was slower in high external K^+ at all investigated voltages. Because the K^+ equilibrium potential was close to –80 mV in mammalian Ringer's solution no tail current could be seen at this repolarization voltage (Fig. 3B). The slowing of deactivation by increasing extracellular K^+ was confirmed in five other cells (data not shown).

We concluded from these experiments that increasing the extracellular K^+ concentration slowed the deactivation in mutant channels too. We therefore investigated deactivation in the mutant channels compared with the wild-type in an external solution with high K^+. Figure 4A shows examples of tail currents of the three channel types after repolarization to –70 mV in high K^+ bathing solution. It can be seen from these records that both mutant channels deactivate faster than the wild-type Kv1.1 channels. The deactivation time constant, τ_t, was 59.0 ms for the wild-type, 8.2 ms for the F184C mutant channel and 1.9 ms for the V408A mutant channel. In additional experiments, we used different repolarization voltages and determined τ_t at each repolarization voltage. Data from several cells were averaged and the means of the time constants obtained from these tail currents were plotted against the repolarization voltages (Fig. 4B). Deactivation was fastest at all voltages in the V408A channels compared with wild-type, and the F184C deactivation time course was in between that of wild-type and V408A mutant channels. To exclude the possibility that the differences were due, at least in part, to the high external potassium concentration used in our experiments, we repeated the experiment shown in Fig. 4A in normal mammalian Ringer's solution at one repolarization potential. The results are shown in Table 1. V408A mutant channels deactivated in normal mammalian Ringer's solution at –70 mV ~20 times faster than wild-type channels, whereas the F184C mutant channels deactivated ~2 times faster than wild-type channels.

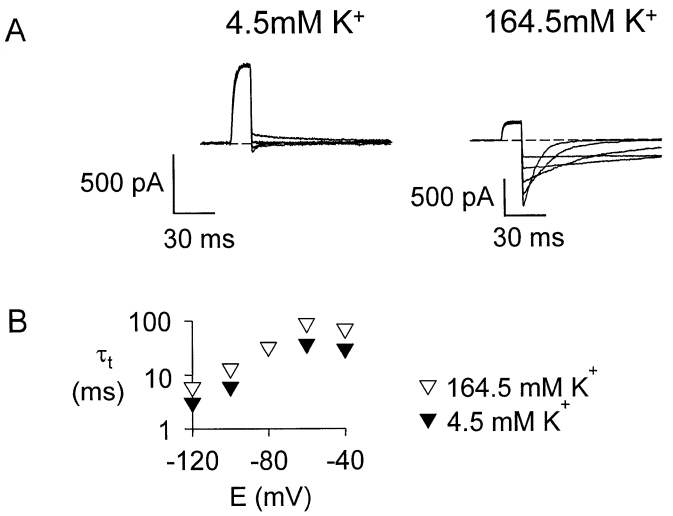

FIG. 3. Effect of $[K^+]_o$ on the deactivation of wild-type Kv1.1 channels. (A) Tail currents were elicited in response to different repolarization steps between –120 and –40 mV in 20-mV increments after a 15-ms prepulse to 40 mV in normal mammalian Ringer's solution with 4.5 mM K^+, and in K^+-bathing solution (164.5 mM K^+). The interpulse interval was 30 s. (B) Tail currents obtained from the records shown in A were fitted with an exponential function, and the resulting deactivation time constants, τ_t, were plotted against the repolarizing potential. Tail currents after repolarization to –80 mV in normal mammalian Ringer's solution were too small for curve-fitting.

Inactivation

Besides activation and deactivation, inactivation is another important property with respect to physiological function. Kv1.1 wild-type channels showed little C-type inactivation and no N-type inactivation when expressed *in vitro* with no additional subunits (Stühmer *et al*., 1989; Grissmer *et al*., 1994). V408A mutant channels, however, were reported to show C-type inactivation three to four times faster than the wild-type when expressed in *Xenopus* oocytes (Adelman *et al*., 1995; D'Adamo *et al*., 1998). Since C-type inactivation is influenced by intracellular constituents of the pipette solution and, in particular, becomes faster if the pipette solution contains KF (Cahalan *et al*., 1985), we used K^+-aspartate in our pipette solution for the investigation of the inactivation properties of the V408A mutant channels compared with wild-type channels. Figure 5A shows a representative experiment for determining the inactivation in Kv1.1 channels. V408A channels inactivated faster compared with wild-type channels and inactivation was almost complete after the 10-s depolarizing pulse (Fig. 5A), whereas F184C channels inactivated like the wild-type Kv1.1 channels (data not shown). Inactivation time constants, τ_h, were obtained by fitting the decay of the current amplitude during the depolarizing pulse to a monoexponential function. This yielded τ_h values for wild-type and V408A mutant channels of ~12 and ~4 s, respectively. To determine the voltage dependence of τ_h, we depolarized the channels to different potentials (from 0 to 50 mV), obtained τ_h values as described above and plotted the resulting τ_h values against the different depolarization voltages (Fig. 5). V408A mutant channels inactivated ~3 times faster than wild-type channels independent of the applied depolarization voltage in this range. This was similar to results obtained when the channels were expressed in *Xenopus* oocytes (Adelman *et al*., 1995; D'Adamo *et al*., 1998).

Selectivity

To characterize mutant Kv1.1 channels further, experiments with different extracellular solutions, containing only one species of permeant ion (K^+, Rb^+, or NH_4^+) were performed. The three types of channels were activated by short depolarizations to 40 mV and then repolarized to voltages in the range of –160 to 40 mV. Amplitudes of instantaneous tail currents were determined and plotted against the applied repolarization voltages (Fig. 6). Current–voltage relations for K^+ or Rb^+ in the external solution showed little inward rectification in all three channel types. However, the solution containing NH_4^+ showed stronger inward rectification. From plots as shown in Fig. 6, reversal potentials (E_{rev}) for the different bath solutions were obtained as described in the legend to Fig. 6. The means of reversal potentials obtained from different experiments are summarized in Table 2. The measured reversal potentials in the K^+-bathing solution were close to the reversal potential predicted by the Nernst equation in all three types of channels. In contrast to NH_4^+, Rb^+ shifted the reversal potential only slightly in the negative direction (see Fig. 6 and Table 2).

Permeability ratios (P_X/P_K) were calculated from the shift in reversal potentials ΔE_{rev} between solutions ($\Delta E_{rev} = E_{revX} - E_{revK}$), using a version of the Goldman–Hodgkin–Katz equation (see Hille, 1992):

$$\Delta E_{rev} = (RT/F)\ln\{P_x[X^+]_o/P_K[K^+]_o)\} \quad (1)$$

with the usual constants R, T and F, and $[X^+]_o$ and $[K^+]_o$ the concentrations of X and K^+, respectively, in bathing solution. The

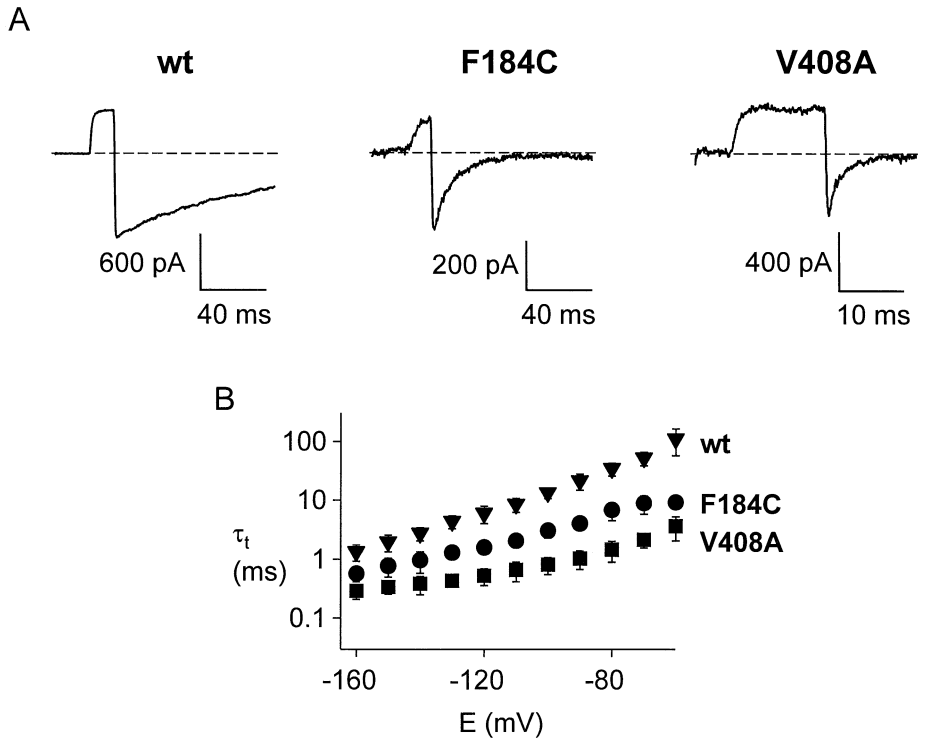

FIG. 4. Deactivation of Kv1.1 wild-type, F184C and V408A channels in a K^+-bathing solution (164.5 mM K^+). (A) Tail currents were elicited in response to repolarization to –70 mV after a 15-ms prepulse to 40 mV. Note the different time scale for currents through V408A mutant channels. (B) The mean ± SD of deactivation time constants τ_t of 5–12 measurements for each channel type were plotted against the repolarization potential. To obtain τ_t, tail currents were similarly elicited as described in (A). Time constants τ_t were results of single monoexponential fits.

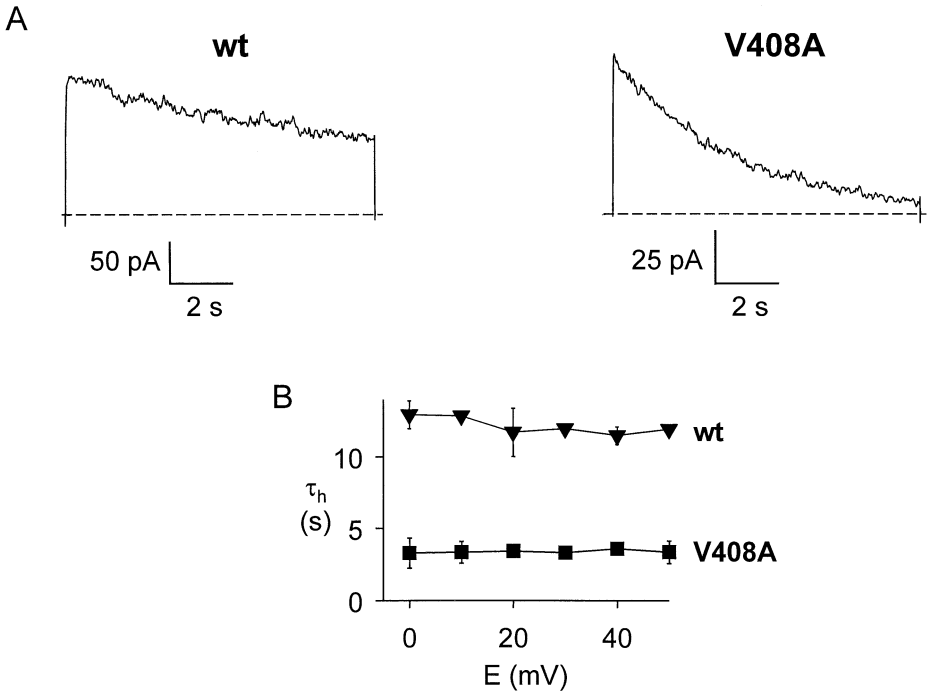

FIG. 5. Inactivation of wild-type and V408A mutant channels. (A) Whole-cell currents were elicited in response to a 10-s depolarizing voltage step to 40 mV. (B) The mean ± SD of the inactivation time constants τ_h of one to five measurements for each voltage and for each channel type were plotted against depolarization voltages. Currents were elicited as described in A, but to additional voltages between 0 and 50 mV (10-mV increments; depolarization every 60 s) and the decays of currents during the 10-s pulses were fitted with single monoexponential functions. The values of the inactivation time constants τ_h at 20 and 40 mV represent five independent measurements. That at 30 mV in V408A is one single measurement. In some cases, SDs were smaller than the symbols. The lines between data points were drawn for clarity.

calculated permeability ratios ($P_X : P_K$) was K^+: Rb^+: NH_4^+ = 1 : 0.8 : 0.1, without significant differences among the three channel types (see Table 2). Conductances, g, were derived from slopes of linear fits through data points between –20 and 0 mV for K^+ and Rb^+, respectively, and between –100 and –70 mV for the NH_4^+-containing bathing solution. For comparison, g_X, calculated from measurements of single cells, was normalized and means of measurements from different cells are shown in Table 2. The conductances of all three channel types were unaltered by substitution of K^+ for Rb^+. Interestingly, inward currents carried by NH_4^+ were larger compared with K^+ outward currents in all three channel types (compare amplitudes of inward currents in NH_4^+ bathing solution at potentials below E_{rev} with those above E_{rev} in Fig. 6) similar to results of Shapiro & DeCoursey (1991) who investigated *l*-type K^+ currents in T lymphocytes, later classified as currents through Kv3.1 channels (Grissmer *et al.*, 1992a).

Single-channel conductance

To investigate if the different maximum conductances (see Table 1) in cells injected with either wild-type- or F184C-cRNA, respectively,

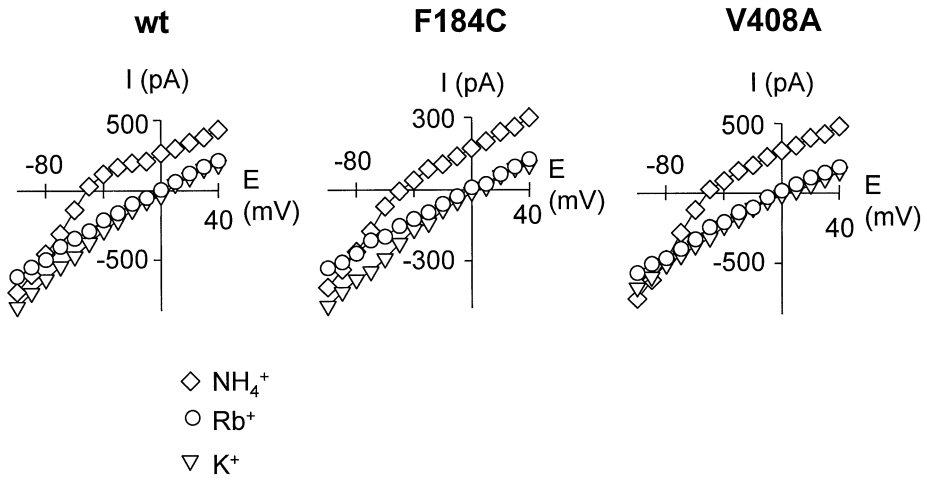

FIG. 6. Effect of monovalent cations on current through wild-type and mutant Kv1.1 channels. Tail currents were elicited as described in Fig. 3, with repolarizations from –100 up to 40 mV, in 10-mV increments every 20 s. The amplitudes of the instantaneous tail currents in the presence of different cations in the bathing solution were plotted against the repolarization potentials. The diagrams show measurements of single cells of wild-type, F184C and V408A mutants. The lines between data points were drawn for clarity.

TABLE 2. Selectivity of Kv1.1 wild-type and mutant channels

	Wild-type *h*Kv1.1 channel		F184C *h*Kv1.1 channel		V408A *h*Kv1.1 channel	
Reversal potential, E_{rev} (mV)						
K^+/K^+ solution*	3.7 ± 3.0	(9)	3.8 ± 1.9	(6)	2.3 ± 4.3	(6)
Rb^+/K^+ solution*	–0.4 ± 1.9	(8)	0.5 ± 2.7	(4)	–0.7 ± 0.4	(4)
NH_4^+/K^+ solution*	–50.2 ± 2.0	(8)	–50.3 ± 1.9	(3)	–52.7 ± 1.7	(3)
Permeability ratio						
$Rb^+ : K^+$	0.8 ± 0.1	(8)	0.8 ± 0.05	(5)	0.8 ± 0.04	(4)
$NH_4^+ : K^+$	0.1 ± 0.01	(8)	0.1 ± 0.01	(3)	0.1 ± 0.01	(3)
Relative conductance (g_X/g_K)						
$X = Rb^+$	0.9 ± 0.2	(5)	1.0 ± 0.1	(4)	1.0 ± 0.1	(4)
$X = NH_4^+$	1.9 ± 0.3	(5)	2.1 ± 0.6	(3)	2.0 ± 0.4	(4)

Values given are mean ± SD, with the number of investigated cells in parenthesis. *Bathing/pipette solution.

were due to different single-channel conductances, we measured single-channel currents of F184C in comparison with wild-type cells (Fig. 7). Depolarizations to different voltages elicited single-channel currents of different amplitudes (Fig. 7A). To quantify and determine the amplitudes of open channels we generated amplitude histograms (Fig. 7B) and fitted Gaussian equations to the data to get the mean amplitudes of open or closed channels (leak current). The differences between these two amplitudes (Fig. 7B) obtained at different potentials were plotted against the depolarization voltage (Fig. 7C). A line was fitted through the data points and the slope of the line yielded the single-channel conductance γ of 12 and 13 pS for wild-type and F184C mutant channels, respectively (Fig. 7C). In addition to the voltage steps performed in Fig. 7A, we continuously changed the voltage to elicit ramp currents. The resulting ramp current traces were superimposed into Fig. 7C. The current amplitudes of the open channels elicited through voltage ramps confirmed the single conductances obtained through the amplitudes derived from histograms. Table 1 summarizes three independent measurements of γ obtained in the described way for wild-type and F184C channels. The values of 12 ± 1 and 13 ± 1 pS for wild-type and F184C, respectively, were not significantly different. In addition, we calculated, from the current traces shown in Fig. 7A, the open probability as the percentage of time the channel spend in the open state compared with the total time of the depolarizations of the wild-type and the F184C mutant channels at strong depolarizations (50 mV), and obtained a similar open probability of 0.75, indicating that the reduced current amplitude observed in whole cell recordings of the mutant F184C channels compared with wild-type channels was mainly due to a reduced number of functional channels at the plasma membrane, and not due to a change in single-channel conductance or open probability of the channel.

Pharmacology

Extracellularly applied TEA^+ is a well known blocker of current through Kv1.1 channels with an IC_{50} value, a $[TEA^+]_o$ that blocks half the channels, of ~0.3 mM (Stühmer *et al*., 1989; Grissmer *et al*., 1994). To be able to compare the pharmacological properties of the mutant channels with the wild-type Kv1.1 channels we re-examined the IC_{50} values for $[TEA^+]_o$ to block current through the wild-type Kv1.1 channels and compared this value with those obtained from the mutant channels. IC_{50} values for $[TEA^+]_o$ to block current through wild-type Kv1.1 channels were 0.34 + 0.02 mM ($n = 4$) (data not shown). For the mutant channels we obtained IC_{50} values for $[TEA^+]_o$ block of 0.34 + 0.03 mM ($n = 3$) for the V408A channels and 0.33 mM for the F184C channel ($n = 1$), suggesting that the mutations did not effect the structure of the extracellular mouth of the channel protein responsible for the action of extracellularly applied TEA^+.

Treatment of EA-1 patients with acetazolamide has been reported to be helpful in some cases (Brunt & van Weerden, 1990; Lubbers *et al*., 1995; Comu *et al*., 1996). One possible explanation for this effect could be that acetazolamide interacts with the mutant channels to normalize their function. In order to investigate this possibility in more detail we applied 1 mM acetazolamide to wild-type, F184C and V408A mutant Kv1.1 channels for up to 30 min. This procedure was

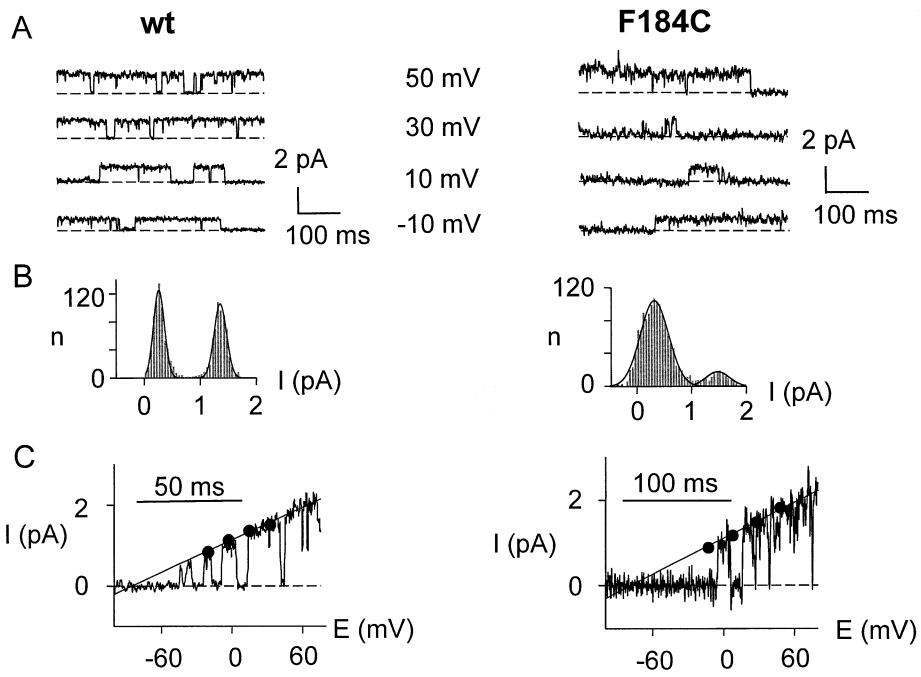

FIG. 7. Single-channel currents of wild-type and F184C mutant Kv1.1 channels in the outside-out configuration. (A) Single-channel currents were elicited in response to repetitive depolarizations to the indicated voltages, and example traces are shown for wild-type and F184C mutant Kv1.1 channels. (B) Examples of amplitude histograms of the 10 mV traces shown in (A) were plotted to obtain the current amplitudes (I) at this voltage. The lines represent Gaussian fits, and the differences of the midpoints of the two bell shaped curves in every histogram gave the value for I. (C) Currents of the same patch were elicited by continuously changing the voltage from –100 to 80 mV in 100 or 200 ms, respectively, and plotted against the ramp voltage. The filled circles in C represent I at different voltages, obtained by the method described in B; the straight line plots represent linear regression fits to these voltage data points. The single-channel conductances γ were obtained from the regression line slopes; they were 12 and 13 pS for the wild-type and F184C mutant channel, respectively.

without any effect on activation, deactivation, inactivation and maximum current of wild-type, F184C and V408A currents (data not shown) suggesting that acetazolamide did not directly interact with the channel protein to normalize function.

Discussion

Our results confirm and extend earlier experiments with similar mutations, but done in another *in vitro* expression system (Adelman *et al*., 1995; D'Adamo *et al*, 1998; Zerr *et al*., 1998). Diminished maximum current amplitudes of mutant compared with wild-type currents in injected cells could be caused either by a reduction in single-channel current amplitudes and/or by a reduction of the total number of functional channels in the cell membrane. We excluded the former for F184C channels, as the single-channel conductances of wild-type and F184C mutants were similar (Fig. 7, Table 1). The values of ~ 12 pS were in good agreement with former single-channel studies of Kv1.1 wild-type channels by Stühmer *et al*. (1989) and Grissmer *et al*. (1994). Zerr *et al*. (1998) estimated similar protein levels for F184C, V408A and wild-type in the total membrane fraction of *Xenopus* oocytes and they concluded from their coinjection studies of wild-type subunits with TEA^+-insensitive EA-1 mutants ('TEA^+-tagged' mutants) that the intracellular transport to the cell surface of both these mutants may be hindered. Our single-channel experiments, at least for the F184C mutant channels, do support this view, although we can not exclude the possibility that non functional mutant subunits may reach the cell surface with the same transport speed as wild-type subunits.

The parameters of channel activation and deactivation determined by us were similar to those obtained from oocytes (Adelman *et al*., 1995; D'Adamo *et al*., 1998; Zerr *et al*., 1998), with minor differences probably due to differences in the expression system. The finding, for example, that deactivation was faster in F184C channels compared with wild-type is in contrast to findings of Adelman *et al*. (1995) and Zerr *et al*. (1998) who found similar (Adelman *et al*., 1995) or even slower (Zerr *et al*., 1998) deactivation time courses in the F184C mutant channels. The difference in the deactivation time constants between wild-type and F184C mutant channels might be due to the difference in the voltage dependence of activation.

The voltage-independent acceleration of C-type inactivation of V408A mutant compared with wild-type channels by a factor of ~ 3 is similar to results of Adelman *et al*. (1995) and D'Adamo *et al*. (1998). Koren *et al*. (1990) depolarized mammalian cells (Sol-8 cells) containing *rat* Kv1.1 channels over periods of 100 s, and determined two voltage-independent inactivation time courses with time constants of ~ 7 and ~ 40 s. Our depolarizations of 10 s duration are very short compared with those by Koren *et al*. (1990) and we could therefore not exclude a second, slower inactivation time course. However, our curve-fits with a steady state current of zero were close to the data, so that the contribution of a second very slow inactivation would be negligible under our conditions.

The acceleration of the inactivation process of V408A mutant compared with wild-type channels is of particular interest, as C-type inactivation is explained by a constriction mechanism of the outer mouth of the channel vestibule (Yellen *et al*., 1994; Panyi *et al*., 1995). It seems that the V408A mutation enables the channel to undergo a faster inactivation, thereby indicating that the inner part of the pore takes part in the conformational change during C-type inactivation. If the residue 408 in Kv1.1 channels could influence conformational changes of the extracellular vestibulum during inactivation, then the shape of the vestibulum could be influenced by this particular mutation, leading to a different affinity for compounds known to interact with this region. Adelman *et al*. (1995) found small differences in the blocking effect of TEA^+ in the

F184C and V408A mutants compared with the wild-type. However, we could not find any difference in the IC_{50} for TEA among the mutant and the wild-type channels, suggesting similar vestibule shapes among the tested channel types.

Since V408 resides in the C-terminal part of the sixth transmembrane domain, which comprises part of the inner portion of the pore (Choi *et al*., 1993; Aiyar *et al*., 1994; Lopez *et al*., 1994), it could have been possible that the V408A mutation caused a change in ion conduction or selectivity. However, in all three channel types under investigation (wild-type, V408A and F184C) we did not find any evidence for a change in either selectivity or conductance compared with the wild-type.

Because the molecular mechanism underlying the therapeutic effect of acetazolamide in some EA-1 patients is unknown, we tested the effect of 1 mM of this compound on currents through Kv1.1 wild-type and mutant channels. However, we could not find any differences in activation, current amplitude, deactivation or inactivation in the presence of the drug, thereby excluding a direct effect of acetazolamide on Kv1.1 channels in this concentration. One possible explanation for why the treatment of acetazolamide can only relieve the symptoms in some patients and not in others, and why acetazolamide had apparently no effect on current through either wild-type or the V408A or F184C mutant channels, could be that only some of the mutated channels (not V408A or F184C) are responsive to treatment by acetazolamide.

Our data indicate that a decreased contribution of Kv1.1 mutants to repolarization of motoneurons, by fewer functional channels, slower activation, activation at more depolarized potentials (F184C), faster deactivation (F184C, V408A) and/or an increased inactivation (V408A) may be the cause of the myokymic discharges. In normal myelinated axons, the juxtaparanodally located Kv1.1 channels do not contribute to the repolarization. Regenerating myelinated axons, however, have a distinct Kv1.1 channel distribution with channels in the nodal membrane (Rasband *et al*., 1998). The treatment of regenerating axons with 4-aminopyridine known to block Kv1.1 channels (and the often similarly distributed Kv1.2 channels) elicited bursting activity after a single stimulus (Kocsis *et al*., 1982). Thus Kv1.1 channels with altered functions seem to be only one of the prerequisites to elicit repetitive discharges, a second one is the electrical accessibility of Kv1.1 channels, e.g. during de- or remyelinating processes.

The site of cerebellar action of mutant Kv1.1 channels responsible for the ataxic episodes is not known. Kv1.1 channels were stained in nearly all parts of the cerebellum with very intense staining in the granular cell layer (Wang *et al*., 1994; Veh *et al*., 1995; Rhodes *et al*., 1997). Only animal models with mutations responsible for EA-1 could determine the site of action and the particular function of Kv1.1 channels leading to paroxysmal disturbances of coordination.

Another interesting question concerns the restriction of symptoms to coordination in EA-1, as Kv1.1 channels have been found in almost all regions of the brain and also in peripheral sensory nerves (Veh *et al*., 1995; Rasband *et al*., 1998). The investigation of intracellular modifiers of mutant Kv1.1 channels such as phosphorylation or interaction with β-subunits, and the study of heteromultimeric assembly of mutant subunits with other Kv1.x subunits could help to solve this question.

Acknowledgements

The authors would like to thank Ms Katharina Ruff and Ms Christine Hanselmann for their excellent technical support; Dr Mark Tanouye for his generous gift of the *h*Kv1.1 channel; and Dr Heike Jäger for help with the generation of the mutants of *h*Kv1.1 channel. This work was supported by grants from the DFG (Gr848/4–2) and the BMBF (Interdisciplinary Center for Clinical Research, IZKF Ulm, B1).

Abbreviations

EA-1, episodic ataxia type 1; E_{rev}, reversal potential; *g*, conductance; γ, single-channel conductance; *h*Kv1.1, human Kv1.1 gene; *k*, gradient of the voltage-dependence curve; *m*Kv1.1, mouse Kv1.1 gene; P_X/P_K, permeability ratio; RBL, rat basophilic leukaemia cell line; τ_h, inactivation time constant; τ_n, activation time constant; τ_t, deactivation time constant; TEA^+, tetraethylammonium.

References

Adelman, J.P., Bond, C.T., Pessia, M. & Maylie, J. (1995) Episodic ataxia results from voltage-dependent potassium channels with altered functions. *Neuron*, **15**, 1449–1454.

Aiyar, J., Nguyen, A.N., Chandy, K.G. & Grissmer, S. (1994) The P-region and S6 of Kv3.1 contribute to the formation of the ion conduction pathway. *Biophys. J.*, **67**, 2261–2264.

Beckh, S. & Pongs, O. (1990) Members of the RCK potassium channel family are differentially expressed in the rat nervous system. *EMBO J.*, **9**, 777–782.

Bretschneider, F., Wrisch, A., Lehmann-Horn, F. & Grissmer, S. (1998) Electrophysiological Characterization of human Kv1.1 potassium channels with point mutations causing episodic ataxia type 1. *Pflügers Arch.*, **435**, R93 (A).

Browne, D.L., Brunt, E.R., Griggs, R.C., Nutt, J.G., Gancher, S.T., Smith, E.A. & Litt, M. (1995) Identification of two new KCNA1 mutations in episodic ataxia/myokymia families. *Hum. Mol. Genet.*, **4**, 1671–1672.

Browne, D.L., Gancher, S.T., Nutt, J.G., Brunt, E.R., Smith, E.A., Kramer, P. & Litt, M. (1994) Episodic ataxia/myokymia syndrome is associated with point mutations in the human potassium channel gene, KCNA1. *Nat. Genet.*, **8**, 136–140.

Brunt, E.R. & van Weerden, T.W. (1990) Familial paroxysmal kinesigenic ataxia and continuous myokymia. *Brain*, **113**, 1361–1382.

Cahalan, M.D., Chandy, K.G., DeCoursey, T.E. & Gupta, S. (1985) A voltage-gated potassium channel in human T-lymphocytes. *J. Physiol.*, **358**, 197–237.

Chandy, K.G., Williams, C.B., Spencer, R.H., Aguilar, B.A., Ghanshani, S., Tempel, B.L. & Gutman, G.A. (1990) A family of three mouse potassium channel genes with intronless coding regions. *Science*, **247**, 973–975.

Choi, K.L., Mossman, C., Aube, J. & Y.e.llen, G. (1993) The internal quaternary ammonium receptor site of Shaker potassium channels. *Neuron*, **10**, 533–541.

Comu, S., Giuliani, M. & Narayanan, V. (1996) Episodic ataxia and myokymia syndrome: a new mutation of potassium channel gene Kv1.1. *Ann. Neurol.*, **40**, 684–687.

D'Adamo, M.C., Liu, Z., Adelman, J.P., Maylie, J. & Pessia, M. (1998) Episodic ataxia type-1 mutations in the hKv1.1 cytoplasmic pore region alter the gating properties of the channel. *EMBO J.*, **17**, 1200–1207.

Eccleston, E., Leonard, B.J., Lowe, J.S. & Welford, H.J. (1973) Basophilic leukemia in the albino rat and a demonstration of the basopoietin. *Nature New Biol.*, **244**, 73–76.

Gancher, S.T. & Nutt, J.G. (1986) Autosomal dominant episodic ataxia: a heterogeneous syndrome. *Mov. Disord.*, **1**, 239–253.

Grissmer, S., Ghanshani, S., Dethlefs, B., McPherson, J.D., Wasmuth, J.J., Gutman, G.A., Cahalan, M.D. & Chandy, K.G. (1992b) The *Shaw*-related potassium channel gene, Kv3.1, on human chromosome 11, encodes the type *l* K^+ channel in T cells. *J. Biol. Chem.*, **267**, 20971–20979.

Grissmer, S., Lewis, R.S. & Cahalan, M.D. (1992a) Ca^{2+}-activated K^+ channels in a human leukemic T-cell line. *J. Gen. Physiol.*, **99**, 63–87.

Grissmer, S., Nguyen, A.N., Aiyar, J., Hanson, D.C., Mather, R.J., Gutman, G.A., Karmilowicz, M.J., Auperin, D.D. & Chandy, K.G. (1994) Pharmacological characterization of five cloned voltage-gated K^+ channels, types Kv1.1, 1.2, 1.3, 1.5, and 3.1, stably expressed in mammalian cell lines. *Mol. Pharmacol.*, **45**, 1227–1234.

Grissmer, S., Nguyen, A.N. & Cahalan, M.D. (1993). Calcium-activated potassium channels in resting and activated human T lymphocytes. Expression levels, calcium dependence, ion selectivity, and pharmacology. *J. Gen. Physiol.*, **102**, 601–630.

Hamill, O.P., Marty, A., Neher, E., Sakmann, B. & Sigworth, F.J. (1981)

Improved patch-clamp techniques for high-resolution current recording from cells and cell-free membrane patches. *Pflügers Arch.*, **391**, 85–100.
Hanson, P.A., Martinez, L.B. & Cassidy, R. (1977) Contractures, continuous muscle discharges, and titubation. *Ann. Neurol.*, **1**, 120–124.
Hille, B. (1992) *Ionic Channels of Excitable Membranes, 2nd edn.* Sinauer Associates, Sunderland, MA, USA.
Jäger, H., Rauer, H., Nguyen, A.N., Aiyar, J., Chandy, K.G. & Grissmer, S. (1998). Regulation of mammalian *Shaker*-related K^+ channels: evidence for non-conducting closed and non-conducting inactivated states. *J. Physiol., 506.*, **2**, 291–301.
Klumpp, D.J., Farber, D.B., Bowes, C., Song, E.J. & Pinto, L.H. (1991) The potassium channel MBK1 (Kv1.1) is expressed in the mouse retina. *Cell Mol. Neurobiol.*, **11**, 611–622.
Kocsis, J.D., Waxman, S.G., Hildebrand, C. & Ruiz, J.A. (1982) Regenerating mammalian nerve fibers: changes in action potential waveform and firing characteristics following blockade of potassium conductance. *Proc. R. Soc. Lond. B. Biol. Sci.*, **217**, 77–87.
Koren, G., Liman, E.R., Logothetis, D.E., Nadal Ginard, B. & Hess, P. (1990) Gating mechanism of a cloned potassium channel expressed in frog oocytes and mammalian cells. *Neuron*, **4**, 39–51.
Laube, G., Röper, J., Pitt, J.C., Sewing, S., Kistner, U., Garner, C.C., Pongs, O. & Veh, R.W. (1996) Ultrastructural localization of *Shaker*-related potassium channel subunits and synapse-associated protein 90 to septate-like junctions in rat cerebellar Pinceaux. *Brain Res. Mol. Brain Res.*, **42**, 51–61.
Litt, M., Kramer, P., Browne, D., Gancher, S., Brunt, E.R., Root, D., Phromchotikul, T., Dubay, C.J. & Nutt, J. (1994) A gene for episodic ataxia/myokymia maps to chromosome 12p13. *Am. J. Hum. Genet.*, **55**, 702–709.
Lopez, G.A., Jan, Y.N. & Jan, L.Y. (1994) Evidence that the S6 segment of the *Shaker* voltage-gated K^+ channel comprises part of the pore. *Nature*, **367**, 179–182.
Lubbers, W.J., Brunt, E.R., Scheffer, H., Litt, M., Stulp, R., Browne, D.L. & van Weerden, T.W. (1995) Hereditary myokymia and paroxysmal ataxia linked to chromosome 12 is responsive to acetazolamide. *J. Neurol. Neurosurg. Psychiatry*, **59**, 400–405.
Mi, H., Deerinck, T.J., Ellisman, M.H. & Schwarz, T.L. (1995) Differential distribution of closely related potassium channels in rat Schwann cells. *J. Neurosci.*, **15**, 3761–3774.
Neher, E. (1992) Correction for liquid junction potentials in patch clamp experiments. *Meth. Enzymol.*, **207**, 123–131.
Panyi, G., Shi, G., Tu, L. & Deutsch, C. (1995) C-type inactivation of a voltage-gated K^+ channel occurs by a cooperative mechanism. *Biophys. J.*, **69**, 896–903.
Rasband, M.N., Trimmer, J.S., Schwarz, T.L., Levinson, S.R., Ellisman, M.H., Schachner, M. & Shrager, P. (1998) Potassium channel distribution, clustering, and function in remyelinating rat axons. *J. Neurosci.*, **18**, 36–47.
Rauer, H. & Grissmer, S. (1996) Evidence for an internal phenylalkylamine action on the voltage-gated potassium channel Kv1.3. *Mol. Pharmacol.*, **50**, 1625–1634.
Rhodes, K.J., Strassle, B.W., Monaghan, M.M., Bekele Arcuri, Z., Matos, M.F. & Trimmer, J.S. (1997) Association and colocalization of the $Kv\beta_1$- and $Kv\beta_2$-subunits with Kv1 α-subunits in mammalian brain K^+ channel complexes. *J. Neurosci.*, **17**, 8246–8258.
Roberds, S.L. & Tamkun, M.M. (1991) Cloning and tissue-specific expression of five voltage-gated potassium channel cDNAs expressed in rat heart. *Proc. Natl Acad. Sci. U.S.A.*, **88**, 1798–1802.
Scheffer, H., Brunt, E.R.P., Mol, G.J.J., van der Vlies, P., Stulp, R.P., Verlind, E., Mantel, G., Averyanov, Y.N., Hofstra, R.M.W. & Buys, C.H.C.M. (1998) Three novel KCNA1 mutations in episodic ataxia type I families. *Hum. Genet.*, **102**, 464–466.
Shapiro, M.S. & DeCoursey, T.E. (1991) Permeant ion effects on the gating kinetics of the type *l* potassium channel in mouse lymphocytes. *J. Gen. Physiol.*, **97**, 1251–1278.
Stühmer, W., Ruppersberg, J.P., Schröter, K.H., Sakmann, B., Stocker, M., Giese, K.P., Perschke, A., Baumann, A. & Pongs, O. (1989) Molecular basis of functional diversity of voltage-gated potassium channels in mammalian brain. *EMBO J.*, **8**, 3235–3244.
Swenson, R.P. & Armstrong, C.M. (1981) K^+ channels close more slowly in the presence of external K^+ and Rb^+. *Nature*, **291**, 427–429.
Tsaur, M.L., Sheng, M., Lowenstein, D.H., Jan, Y.N. & Jan, L.Y. (1992) Differential expression of K^+ channel mRNAs in the rat brain and down-regulation in the hippocampus following seizures. *Neuron*, **8**, 1055–1067.
VanDyke, D.H., Griggs, R.C., Murphy, M.J. & Goldstein, M.N. (1975) Hereditary myokymia and periodic ataxia. *J. Neurol. Sci.*, **25**, 109–118.
Veh, R.W., Lichtinghagen, R., Sewing, S., Wunder, F., Grumbach, I.M. & Pongs, O. (1995) Immunohistochemical localization of five members of the Kv1 channel subunits: contrasting subcellular locations and neuron-specific co-localizations in rat brain. *Eur. J. Neurosci.*, **7**, 2189–2205.
Wang, H., Kunkel, D.D., Martin, T.M., Schwartzkroin, P.A. & Tempel, B.L. (1993) Heteromultimeric K^+ channels in terminal and juxtaparanodal regions of neurons. *Nature*, **365**, 75–79.
Wang, H., Kunkel, D.D., Schwartzkroin, P.A. & Tempel, B.L. (1994) Localization of Kv1.1 and Kv1.2, two K channel proteins, to synaptic terminals, somata, and dendrites in the mouse brain. *J. Neurosci.*, **14**, 4588–4599.
Yellen, G., Sodickson, D., Chen, T.Y. & Jurman, M.E. (1994) An engineered cysteine in the external mouth of a K^+ channel allows inactivation to be modulated by metal binding. *Biophys. J.*, **66**, 1068–1075.
Zerr, P., Adelman, J.P. & Maylie, J. (1998) Episodic ataxia mutations in Kv1.1 alter potassium channel function by dominant negative effects or haploinsufficiency. *J. Neurosci.*, **18**, 2842–2848.